

Mathematical modelling of angiogenesis

Mark A.J. Chaplain

Department of Mathematics, University of Dundee, Dundee, Scotland, UK

Key words: mathematical modelling, angiogenesis, chemotaxis, haptotaxis

Summary

Angiogenesis, the formation of blood vessels from a pre-existing vasculature, is a process whereby capillary sprouts are formed in response to externally supplied chemical stimuli. The sprouts then grow and develop, driven initially by endothelial cell migration, and organize themselves into a branched, connected network. Subsequent cell proliferation near the sprout-tips permits further extension of the capillaries and ultimately completes the process. Angiogenesis occurs during embryogenesis, wound healing, arthritis and during the growth of solid tumours. In this article we first of all present a review of a variety of mathematical models which have been used to describe the formation of capillary networks and then focus on a specific recent model which uses novel mathematical modelling techniques to generate both two- and three-dimensional vascular structures. The modelling focusses on key events of angiogenesis such as the migratory response of endothelial cells to exogenous cytokines (tumour angiogenic factors, TAF) secreted by a solid tumour; endothelial cell proliferation; endothelial cell interactions with extracellular matrix macromolecules such as fibronectin; capillary sprout branching and anastomosis. Numerical simulations of the model, using parameter values based on experimental data, are presented and the theoretical structures generated by the model are compared with the morphology of actual capillary networks observed in *in vivo* experiments. A final conclusions section discusses the use of the mathematical model as a possible angiogenesis assay.

1. Introduction

Angiogenesis, the formation of blood vessels from a pre-existing vasculature, is a crucial component of many mammalian growth processes. For example, it occurs in early embryogenesis during the formation of the placenta, after implantation of the blastocyst in the uterine wall [1]; it occurs in adult mammals during tissue-repair and wound healing [2]. While these are examples of controlled angiogenesis, by contrast, uncontrolled or excessive blood-vessel formation, is essential for tumourigenesis and is also observed in inflammatory diseases such as arthritis, abnormal neovascularization of the eye, duodenal ulcers, and following myocardial infarction [3–5]. These instances may all be considered as pathological examples of angiogenesis [6]. In each case, however, the well-ordered sequence of events characterizing angiogenesis is the same, beginning with the rearrangement and migration of endothelial cells from a

pre-existing vasculature and culminating in the formation of an extensive branched, connected network of new capillaries [7,8]. In this article we will present a review of the mathematical modelling of angiogenesis, focussing specifically on tumour-induced angiogenesis. The models which are described in the later sections can, however, be easily adapted to examine angiogenesis in controlled settings such as wound healing and embryo implantation [9–11]. Before presenting any mathematical models, we will first begin with a brief overview and description of the key processes involved in angiogenesis.

The first event of tumour-induced angiogenesis involves the cancerous cells of a solid tumour secreting a number of chemicals, collectively known as tumour angiogenic factors, or TAF [3], into the surrounding tissue. These factors (cytokines) diffuse through the tissue (extracellular matrix) thereby creating chemical gradients in the tissue surrounding the tumour. Once the cytokines reach any neighbouring blood vessels,

endothelial cells lining these vessels are stimulated into a sequence of events affecting their migration and proliferation which culminates in the tumour being penetrated by a capillary network of blood vessels.

Firstly, the endothelial cells are induced to synthesize matrix degradative enzymes (proteinases and collagenases) and to degrade the parent venule basement membranes and then migrate through the disrupted membrane towards the tumour [12]. The initial migratory response of the endothelial cells to these angiogenic factors is a chemotactic one [8,13,14], and the cells begin to move out of their parent vessel into the surrounding tissue towards the tumour. Following this initial event, small, finger-like capillary sprouts are formed by accumulation of endothelial cells which are recruited from the parent vessel. The sprouts grow in length due to the migration and further recruitment of endothelial cells [8,14,15] and continue to move toward the tumour directed by the motion of the leading endothelial cell at the sprout-tip. Further sprout extension occurs when some of the endothelial cells of the sprout-wall begin to proliferate. Cell division is largely confined to a region just behind the cluster of mitotically inactive endothelial cells that constitute the sprout-tip. This process of sprout-tip migration and proliferation of sprout-wall cells forms solid strands of endothelial cells within the extracellular matrix. Interactions between the cells and the matrix are very important and directly affect cell migration. Although there are several matrix macromolecules which are known to interact with the endothelial cells, specific interactions between the endothelial cells and fibronectin are known to be very important for migration, with fibronectin having been shown to enhance cell adhesion to the matrix [16–18]. It has been verified experimentally that fibronectin stimulates directional migration of endothelial cells in Boyden chamber assays [19]. These results have demonstrated that fibronectin promotes cell migration up a concentration gradient and the results of [20–22] have further demonstrated that this is a response of the cells to a gradient of adhesiveness of bound fibronectin, termed haptotaxis [23,24]. Therefore, in addition to the chemotactic response of the endothelial cells to the angiogenic cytokines, there is a complementary haptotactic response to the fibronectin present within the extracellular matrix [25].

Initially, the sprouts arising from the parent vessel grow essentially parallel to each other. It is observed that once the finger-like capillary sprouts have reached

a certain distance from the parent vessel, they tend to incline toward each other [8], leading to numerous tip-to-tip and tip-to-sprout fusions known as anastomoses. Such anastomoses result in the fusing of the finger-like sprouts into a network of poorly perfused loops or arcades. Following this process of anastomosis, the first signs of circulation can be recognized and from the primary loops, new buds and sprouts emerge repeating the angiogenic sequence of events and providing for the further extension of the new capillary bed. The production of new capillary sprouts from the sprout-tips is often referred to as sprout branching, and as the sprouts approach the tumour, their branching dramatically increases until the tumour is eventually penetrated, resulting in vascularization.

This process of repeated steps of endothelial cell migration, sprout extension, cell proliferation and loop formation is necessary for the successful vascularization of the tumour. However, it has been demonstrated that, in the absence of endothelial cell proliferation, a restricted capillary network, which stops after a few days and never reaches the tumour, is formed [14].

Tumour-induced angiogenesis provides the crucial link between the avascular phase of solid tumour growth and the more harmful vascular phase, wherein the tumour invades the surrounding host tissue and blood system [26]. Once invasion has occurred, the possibility of the cancer spreading to other parts of the body (metastasis) becomes a reality and is far more difficult to treat clinically. However, these apparently insidious features of tumour-induced angiogenesis are now being used to combat cancer growth and the clinical importance of angiogenesis as a prognostic tool is now recognized. In developing mathematical models of angiogenesis we hope to be able to provide a deeper insight into the underlying mechanisms which cause the process [18]. It is therefore essential that predictive mathematical models are developed which are capable of producing the precise, quantitative *morphological features* of developing blood vessels.

In the next section, we give a brief review of several mathematical models of angiogenesis before describing in more detail some recent work of Chaplain and Anderson [27–30]. This work focusses specifically on the so-called *tissue response unit* [18], which consists of the endothelial cells and their immediate microenvironment of cytokines and matrix molecules. Using this model we will demonstrate the extent to which a (relatively) simple (minimal) mathematical model can replicate the salient features of a growing capillary

network (more generally, any branching, connected network) not merely in a phenomenological, qualitative manner but, more importantly, in a quantitative and predictive manner.

2. Mathematical models of angiogenesis

The scientific study of networks and their function can be traced back as far as Leonardo da Vinci with his beautifully detailed and intricate sketches of human lungs. Perhaps the first mathematical analysis of networks can be found in the classic work of D'Arcy Thompson [31] where he studies '*... a number of interesting points in connection with the form and structure of the blood-vessels...*'. In more recent years several mathematical models, using a variety of applied mathematical techniques, have been developed to describe some of the key features of tumour-induced angiogenesis.

Several models have used the mathematical technique of partial differential equations, and have been able to examine the distribution in space and time of variables such as endothelial cell density, capillary tip and branch density, and angiogenic factor concentration. Models in one space dimension include those of [32–37]. These models deal both with tumour-induced angiogenesis and angiogenesis in wound healing. Although these models are capable of capturing some features of angiogenesis at a 'macroscale', such as average sprout density and network expansion rates, they are unable to provide more detailed information at a 'microscale' concerning the actual structure and morphology of the capillary network and as such were of limited predictive value.

More realistic partial differential equation models of angiogenesis in two space dimensions have been considered by [38–41]. The results of these models permit a more detailed qualitative comparison with *in vivo* observations concerning the spatio-temporal distribution of capillary sprouts within the network. In particular the work of Orme and Chaplain goes some way to examine strategies of anti-angiogenesis. However, even with these models, it is not possible to capture certain important events such as repeated sprout branching and hence the overall dendritic structure of the network. Other two-dimensional models deal with the role of mechanical forces on the developing capillary network [42–44].

In contrast to these deterministic, continuum models, several different types of discrete models, such as coupled map lattice models, fractal models, diffusion limited aggregation models and L-systems, have been used to model the branching morphology of capillary network formation and angiogenesis [45–47].

The model of [48] used a discrete probabilistic framework in two space dimensions, based on stochastic differential equations. This approach had the advantage of enabling the motion of *individual endothelial cells* to be followed. Realistic capillary network structures were generated by incorporating rules for sprout branching and anastomosis. Since parameters were estimated, as far as possible, from available experimental data, this permitted both qualitative and quantitative comparisons with *in vivo* networks to be made. Although the model incorporated random motility and chemotaxis as mechanisms for cell migration, no account was taken of the important interactions between the endothelial cells and the extracellular matrix. The model was also unable to reproduce the fact that there is an increased frequency of branching at the edge of the network as the capillary sprouts get closer to the tumour. This observed feature of tumour-induced angiogenesis has been described as the '*brush border*' effect [14,49,50].

An excellent collection of articles containing several different mathematical models and a variety of the modelling techniques mentioned above used can be found in [51].

In the remainder of this article, we will describe new and recent advances made in modelling tumour-induced angiogenesis. The mathematical model we will present focuses on the interactions between three very important variables involved in tumour-induced angiogenesis; namely, endothelial cells, tumour angiogenic factors (TAF) and fibronectin, each of which has a crucial role to play (cf. *the tissue response unit* [18]).

The morphological events that are involved in new blood-vessel formation have been defined by studies of *in vivo* systems such as the chick chorioallantoic membrane (CAM), animal corneal models and *in vitro* examination of endothelial cell migration and proliferation [52,53]. The particular experimental system upon which we will base our initial mathematical model is that of the implant of a solid tumour in the cornea of a test animal [49,50]. Parameter values used in the model will be based, as far as possible, on estimates obtained from experimental observations.

Once the basic mathematical model has been presented, we will then develop the model still further and use computer simulations of the model to generate a fully 3-dimensional capillary network. It is possible to analyse these theoretical structures for quantitative information such as network expansion rates, loop formation, sprout length and overall network architecture (e.g. vessel area and volume). In final section we discuss the possibility of using the model as the basis for a *quantitative angiogenesis assay* [53].

3. Modelling the tissue response unit

As already mentioned in the previous section, we focus our modelling attention on the so-called *tissue response unit* [18] consisting of endothelial cells, a generic tumour angiogenic factor or TAF (e.g. a cytokine such as VEGF) and a generic matrix macromolecule known to affect cell adhesion (e.g. fibronectin). We denote the endothelial cell density per unit area by n , the angiogenic factor concentration by c and the fibronectin concentration by f .

In developing mathematical models of angiogenesis, we are particularly interested in the *rates of change* of variables with time and how the amount (e.g. concentration, density etc.) of the variables changes from point to point in space. The changes in the variables that we study depend on their spatial position and on time and mathematically we use tools known as partial differential equations to describe these changes. A variable, V , say (e.g. concentration of a cytokine or the number of endothelial cells per unit area/volume, i.e. cell density) will therefore be a function of its spatial coordinates (x, y, z) and time t . We denote this mathematically by writing $V(x, y, z, t)$. To construct a differential equation model we make use of the calculus (which enables us to describe the rate of change of variables) and the law of the conservation of mass. Applying these two rules we can formulate a generic ‘conceptual’ equation describing the rate of change of a substance with respect to time, its migration and its production/decay. Thus, we have:

$$\begin{aligned} \text{rate of change} &= \text{spatial migration} + \text{production} \\ \text{of variable} &\quad - \text{decay/uptake.} \end{aligned}$$

By solving the above equation mathematically, at any given time one can predict how much of the variable (e.g. number of cells, amount of cytokine) is present in one’s system. One may draw an analogy between

the above equation describing a biological population (e.g. of cells, amount of a cytokine) and the population of a country – at any given time the number of people in the country can be calculated from the number of immigrants/emigrants (cf. migration/diffusion) and the number of births/deaths (cf. production/decay).

Turning to our particular problem of angiogenesis, we first consider the mechanisms involved in endothelial cell migration. We assume that the motion of the endothelial cells (at or near a capillary sprout-tip) is influenced by three factors: random motility (analogous to molecular diffusion), chemotaxis in response to TAF gradients in the surrounding connective tissue stroma [54,55] and haptotaxis in response to fibronectin gradients, also present in the surrounding tissue [16,20–22,25].

To derive the TAF equation, we first of all consider the initial event of tumour-induced angiogenesis which is the secretion of TAF by the tumour cells. Once secreted, TAF diffuses into the surrounding corneal tissue and extracellular matrix and sets up a concentration gradient between the tumour and any pre-existing vasculature such as the nearby limbal vessels. As the endothelial cells migrate through the extracellular matrix in response to this steady-state gradient [48], there is some binding of TAF by the endothelial cells [15,56]. We model this process by a simple uptake function.

Fibronectin is known to be present in most mammalian tissue and has been identified as a component of the tissue of the cornea. In addition to this pre-existing fibronectin, it is known that the endothelial cells themselves produce and secrete fibronectin which then becomes bound to the extracellular matrix and does not diffuse [17]. There is also binding of fibronectin to the endothelial cells via integrins as they migrate toward the tumour [17]. Finally, the tissue is degraded by degradative enzymes.

Hence the complete system of partial differential equations describing the interactions of the endothelial cells, angiogenic cytokine and fibronectin is given by:

$$\begin{aligned} \frac{\partial n}{\partial t} &= \overbrace{D_n \nabla^2 n}^{\text{random motility}} - \overbrace{\chi_0 \nabla \cdot (n \nabla c)}^{\text{chemotaxis}} - \overbrace{\rho_0 \nabla \cdot (n \nabla f)}^{\text{haptotaxis}}, \\ \frac{\partial f}{\partial t} &= \overbrace{\omega n}^{\text{production}} - \overbrace{\mu n f}^{\text{binding/degradation}}, \\ \frac{\partial c}{\partial t} &= - \overbrace{\lambda n c}^{\text{uptake/binding}}. \end{aligned} \tag{1}$$

Full details of the model and the various terms of the equations can be found in [27–29].

The above equations are considered to hold on a square spatial domain of side L (representing a square of corneal tissue) with the parent vessel (e.g. limbal vessel) located along one edge and the tumour located on the opposite edge. We assume that the cells, and consequently the capillary sprouts, remain within the domain of tissue under consideration and therefore no-flux boundary conditions are imposed.

Wherever possible parameter values have been estimated from available experimental data. An average distance from a tumour implant to parent vessels in the cornea is between 1 and 2.5 mm [49,50] and we take the lengthscale $L = 2$ mm [48]. The experiments of [54] and [57] on endothelial cell migration in response to angiogenic factors and data from [58] provide us with estimates for D_n and χ_0 , ρ_0 of 10^{-10} cm² s⁻¹ and 2600 cm² s⁻¹ M⁻¹ respectively. Using these parameter values enables us to solve a non-dimensionalized (scaled) version of the system of equations (1) using appropriate numerical simulation techniques (see [27–29] for full details). Figure 1 shows the results of one such simulation where we have attempted to reproduce a corneal implant experiment [49,50]. A small circular tumour is located in the tissue as indicated in the diagram, and a radially symmetric TAF concentration profile (centred around the tumour) is generated within the tissue. This is assumed to be at a high level in the immediate vicinity of the tumour decaying in a radially symmetric manner to lower values on all boundaries and hence creating a gradient. Fibronectin is distributed evenly throughout the entire domain. The parent vessel is located along the left hand boundary (y -axis) and initially there are three regions of endothelial cell density representing areas of capillary sprout growth in response to the TAF concentration gradient.

Figure 1 shows the plots of the endothelial cell density profiles for times 1.5–22.5 days after implantation of the tumour source. The profile at time 1.5 days shows the effect of the circular geometry of the initial TAF concentration profile on the response of the cells, with the outer clusters of endothelial cells initially seen to be moving towards the central cluster. As time goes on, the outer clusters continue to move laterally and two main clusters are then formed around 3–4.5 days. These two clusters subsequently come together to form one large central cluster of high cell density at around 7.5 days. By a time of 15 days we can see that there has been some lateral spread as well as both forward and

backward migration of cells. There is a region of high cell density at the leading edge and also, interestingly, near the parent vessel at $x = 0$. From a time of 18 days (not shown) to a time of $t = 22.5$ days, regions of high cell density appear near the parent vessel and migrate forward and also laterally. By a time of 22.5 days, a small cluster of cells has reached the tumour. At this stage interactions between the endothelial cells and the tumour cells now become important and our model is no longer valid.

Although the results of the model are qualitatively realistic, the model cannot generate the finer detailed structure of a branched network. In the next section we describe a novel mathematical modelling technique which will enable us to achieve this.

3.1. Discrete mathematical modelling of angiogenesis

In order to capture the precise morphological features of the developing capillary network such as individual capillary sprouts, branching and anastomosis, we must develop our mathematical model still further. In this section we describe a recent *discrete* mathematical model of tumour-induced angiogenesis due to [27–29] which enables not only a qualitative but also a quantitative comparison with *in vivo* experimental results. The model is based around the assumption that the motion of an individual endothelial cell located at the tip of a capillary sprout governs the motion of the whole sprout. This is not unreasonable since the remaining endothelial cells lining the sprout-wall are contiguous [8,48].

The technique first of all involves discretizing (using standard finite-difference methods) the partial differential equation in (1) governing the rate of change of endothelial cell density n . This involves approximating our continuous two-dimensional domain $[0, 1] \times [0, 1]$ as a grid of discrete points (with a mesh size between grid points of h), and time (t) by discrete increments of length k . We then use the resulting coefficients of the five-point finite-difference stencil to generate the *probabilities of movement* of an *individual endothelial cell* in response to its local milieu (microenvironment). The resulting equation governing the migration of an endothelial cell has the form:

$$n_{l,m}^{q+1} = n_{l,m}^q P_0 + n_{l+1,m}^q P_1 + n_{l-1,m}^q P_2 + n_{l,m+1}^q P_3 + n_{l,m-1}^q P_4, \quad (2)$$

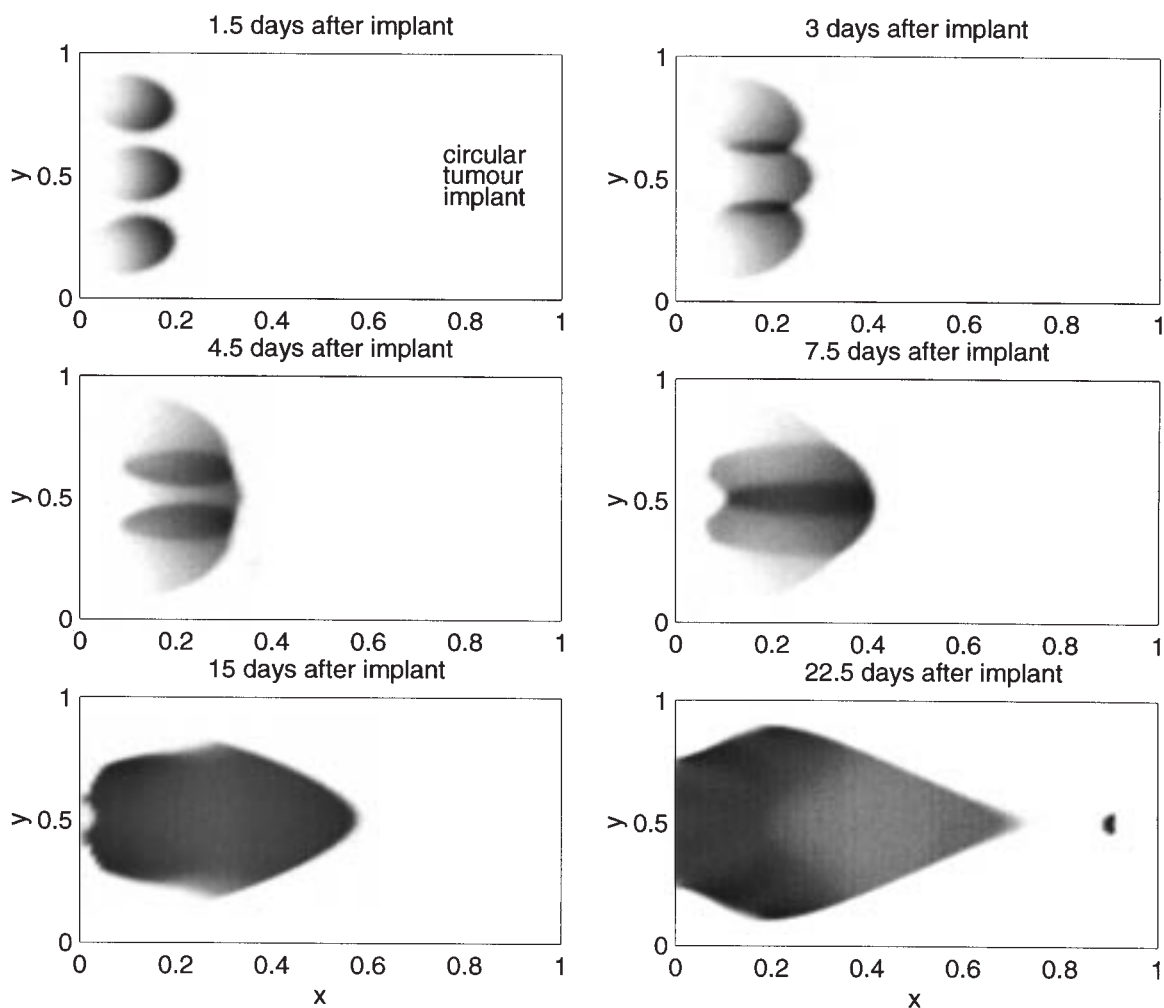


Figure 1. Spatio-temporal evolution of regions of endothelial cell density from a numerical simulation of system (1) representing endothelial cell migration from the parent vessel (left hand edge) toward a circular tumour implant. The initial three areas of high cell density are drawn towards the centre of the domain, where they coalesce and eventually form into one central area with the region of highest cell density located at the leading edge. Colour graduation is directly proportional to cell density, i.e. black is high density and white is low density.

where the subscripts specify the location on the grid and the superscripts the time steps. That is $x = lh$, $y = mh$ and $t = qk$ where l, m, k, q and h are positive parameters.

For our discrete model, we will use the five coefficients P_0 – P_4 from (2) to generate the motion of an individual endothelial cell. These coefficients can be thought of as being proportional to the probabilities of the endothelial cell being stationary (P_0) or moving left (P_1), right (P_2), up (P_3) or down (P_4). The precise forms of P_0 – P_4 are functions of the fibronectin and TAF

concentrations at the neighbouring spatial points of an individual endothelial cell (see [28] for full details) and hence one can see that this discrete model truly permits one to consider the interactions between cells and their microenvironment. The motion of an individual cell at the sprout-tip is therefore governed by its interactions with angiogenic factors and matrix macromolecules in its local microenvironment. In addition we also explicitly incorporate the processes of branching, anastomosis and cell proliferation into the discrete model.

Branching and anastomosis

While there is a good deal of information regarding the actual events of the generation of new sprouts (sprout branching) and the formation of loops (anastomosis), there is no explanation as to the precise mechanisms which cause them [8]. We will assume that the generation of new sprouts (branching) occurs only from existing sprout-tips. It is also reasonable to assume that the newly formed sprouts are unlikely to branch immediately and that there must be a sufficient number of endothelial cells, near the sprout-tip, for new sprouts to form. Thus, in order for branching to be possible:

- (i) the age of the current sprout must be greater than some threshold branching age, i.e. new sprouts must mature for a specified length of time before being able to branch. In the simulations that follow, we found that a threshold branching age of between 20 and 24 h produced simulated networks which were qualitatively similar in morphology to those networks observed *in vivo*.
- (ii) There must be sufficient space locally for a new sprout to form, i.e. branching into a space occupied by another sprout is not possible.

Given that each of the above conditions is satisfied, we assume that each sprout-tip has a probability, P_b , of generating a new sprout (branching) and that this probability is dependent on the local TAF concentration. We therefore adopt a simple *positional information* approach with the rule that as the TAF concentration increases, the probability of generating new sprouts (branching) increases. The branching probabilities are chosen on a qualitative basis, i.e. very little branching occurs initially (near the parent vessel, e.g. limbus), but as the endothelial cells migrate closer to the tumour (at $x = 1$) the number of new sprouts slowly increases. A short distance from the tumour the frequency of branching dramatically increases creating the ‘brush border’ effect.

Anastomosis, the formation of loops by capillary sprouts, is another very important feature of angiogenesis which can be captured explicitly by the discrete model. As the sprouts progress towards the tumour, driven by the movement probabilities of (2), at each time step of the simulation, the endothelial cells at the sprout-tips can move to any of the four orthogonal neighbours on the discrete grid. If upon one of these moves another sprout is encountered, then anastomosis can occur. Experiments have shown that the initial formation of anastomoses occurs at a well-defined distance from the parent vessel [8]. For simplicity, we

assume that as a result of the anastomosis, only one of the original sprouts continues to grow (the choice of which is purely random).

Cell proliferation

As discussed in the introduction, during angiogenesis, there is initially no endothelial cell proliferation. Cells are recruited from the parent vessel and migrate toward the tumour. Approximately 36–48 h into the process, cell mitosis is observed [8,14] and is confined to a region just behind the sprout-tip. Endothelial cell doubling time has been estimated at 18 h [59] and we model the process of cell division in the discrete model by assuming that some of the cells behind the sprout-tip divide (into two daughter cells) every 18 h. We assume that this has the effect of increasing the length of a sprout by approximately one cell length every 18 h. Owing to the inherent randomness of the discrete model, proliferation will occur asynchronously in separate sprouts, as is observed experimentally [8]. This feature is captured by the discrete model since the age of each cell at a sprout-tip is known and this determines when mitosis occurs.

4. Discrete model simulation results

All the simulations of the discrete model were carried out on a 200×200 grid, which is a discretization of the unit square, $[0, 1] \times [0, 1]$, with a space step of $h = 0.005$. Given that our unit of length is 2 mm, this means that h is equivalent to a dimensional length of $10 \mu\text{m}$, i.e. approximately the length of one or two endothelial cells [12].

For the simulations of Figure 2 the parent vessel is located along the left boundary and a tumour is located along the right boundary. We assumed an initial homogeneous distribution of fibronectin throughout domain, and a TAF concentration profile which is high at boundary $x = 1$ (where the tumour cells are located) and low at boundary $x = 0$ (where parent vessel is located). There is thus an initial concentration gradient of TAF across the domain. We assume that there are five capillary sprouts initiated by five endothelial cells located at the sprout-tips.

Figure 2 shows the results of simulating the discrete model as described above, incorporating endothelial cell proliferation, sprout branching and anastomosis with a linear source of tumour cells located at $x = 1$. Cell proliferation is assumed to begin 48 h into the

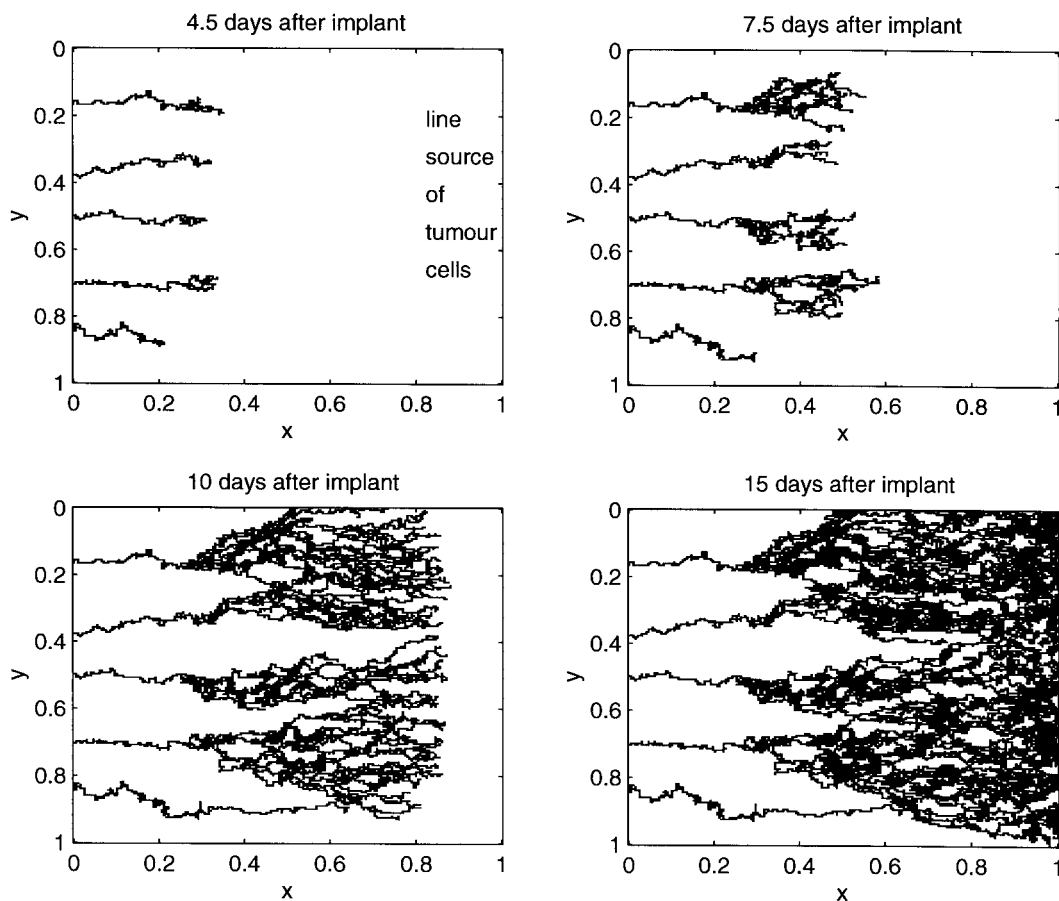


Figure 2. Spatio-temporal evolution of a capillary network from a numerical simulation of the discrete model. The figure shows the migration of endothelial cells at sprout-tips in response to a line source of tumour cells. The parent vessel is located along the left-hand boundary while the tumour cells are located along the right-hand boundary. The cells respond chemotactically to TAF gradients and haptotactically to fibronectin gradients as well as proliferating. As the sprouts grow and migrate, a branched, connected network is formed which connects with the tumour between a time of $t = 10$ –15 days and vascularization is achieved.

process, and cell doubling is assumed to occur every 18h. By 4.5 days sprouts one and two (from the top) have almost formed a loop. By 7.5 days, we see that a well-developed branching network is forming, with proliferation providing additional extension of the sprouts. By 10 days, there are many connections of sprouts and by 15 days, the sprouts have already connected with the tumour.

Figure 3 shows the results of simulating the discrete model (as described above), but this time with a circular tumour implant (shown as the black semi-circle). The initial TAF concentration profile is high around the edge of the tumour and decays away in a radially symmetric manner throughout the rest of the domain. At 4.5 days, we can see that there is already a loop formed by fusion

of the bottom two sprouts and all sprouts are migrating towards the centre of the domain. By 7.5 days, all sprouts have connected in the middle of the domain and further branching and connections occur as the network develops (10 days). By 15 days, the sprouts have connected with the tumour. The results of the model are in excellent quantitative agreement with networks which form in the animal cornea experiments.

While the results of the two-dimensional simulations are in excellent quantitative agreement with the experimental results carried out in animal corneal models [49,50], we know that generally *in vivo* angiogenesis is a fully three-dimensional process. Hence we now finally consider extending the model to 3 spatial dimensions in order to more faithfully represent the actual

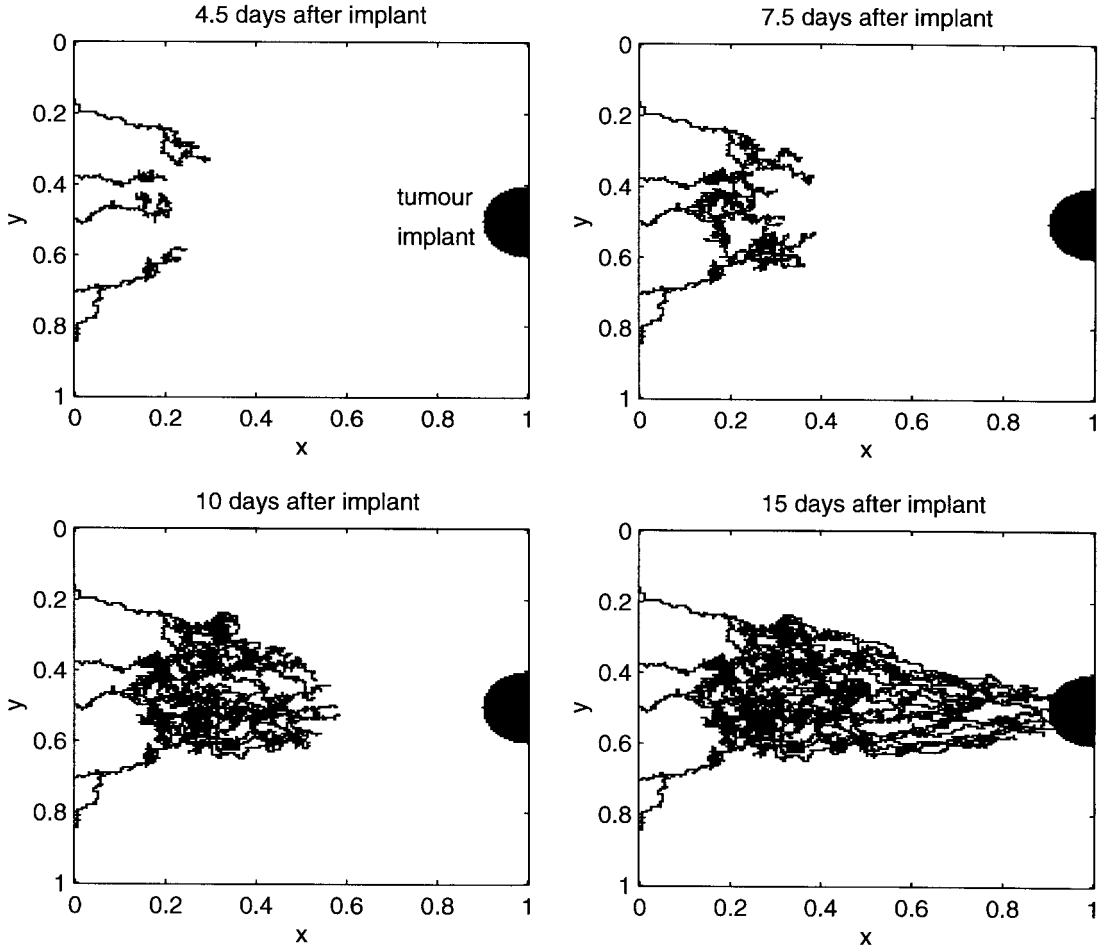


Figure 3. Spatio-temporal evolution of a capillary network from a numerical simulation of the discrete model. The figure shows the migration of endothelial cells at sprout-tips in response to a circular source of tumour cells. The parent vessel is once again located along the left-hand boundary while the circular tumour implant is shown in black at the opposite boundary. The cells respond chemotactically to TAF gradients and haptotactically to fibronectin gradients as well as proliferating. As the sprouts grow and migrate, a branched, connected network is formed. Once again the network connects with the tumour around $t = 15$ days and vascularization is achieved.

in vivo situation. To extend the discrete model to 3 spatial dimensions we simply discretize the spatial terms of the continuous model (1) in three dimensions (i.e. we use a seven point stencil instead of a five point one). We present below the general form of the discrete equation governing the migration of the endothelial cells:

$$n_{l,m,w}^{q+1} = n_{l,m,w}^q P_0 + n_{l+1,m,w}^q P_1 + n_{l-1,m,w}^q P_2 + n_{l,m+1,w}^q P_3 + n_{l,m-1,w}^q P_4 + n_{l,m,w+1}^q P_5 + n_{l,m,w-1}^q P_6, \quad (3)$$

where the subscripts specify the location of an individual cell on the three-dimensional grid and the superscripts denote the time steps. That is $x = lh$,

$y = mh$, $z = wh$ and $t = qk$ where l, m, w, k, q and h are positive parameters.

As with the discrete model in 2 dimensions, we will use the seven coefficients P_0 – P_6 from (3) to generate the motion of an individual endothelial cell in response to its three-dimensional microenvironment. Once again these coefficients can be thought of as being proportional to the probabilities of the endothelial cell being stationary (P_0) or moving west (P_1), east (P_2), north (P_3), south (P_4), up (P_5), or down (P_6). Once again the exact forms of P_0 – P_6 involve functions of the fibronectin and TAF concentrations near an individual endothelial cell.

All the simulations of the three-dimensional discrete model were carried out on a $100 \times 100 \times 100$ grid, which is a discretization of a the unit cube, $[0, 1] \times [0, 1] \times [0, 1]$, with a spatial grid size of $h = 0.01$. In dimensional terms, the cube has sides of length 2 mm, and, as before, one (dimensionless) computational time unit t is equivalent to 1.5 days.

We shall consider the (theoretical) response of new capillaries to both linear (more precisely planar) and spherical tumour sources (representing either a large or small solid tumour implant). In the first simulation (Figure 4) the tumour cells are distributed homogeneously on the bottom face of the cube and this provides a TAF gradient from the bottom face of the cube (high concentration) to the top face of the cube (low concentration). Five initial capillary sprouts are initiated at the top face of the cube and these respond to the

TAF gradient and the fibronectin (initially distributed homogeneously throughout the domain). In the second simulation (Figure 5) a spherical tumour source is positioned at the centre of the unit cube (representing a small spherical tumour or multicell spheroid) with the resulting TAF concentration field assumed to be radially symmetric. There is a high concentration of TAF around the tumour, decaying to a lower concentration on the boundaries. On five out of the six faces of the cube we randomly place 3 initial sprouts, giving a total of 15 capillary sprouts to start the process. Once again the initial fibronectin concentration is assumed to be constant throughout the cube.

Figure 4 shows four snapshots in time of the developing capillary network in response to the planar source of tumour cells on the bottom face of the cube. As can be seen, the sprouts grow, branch and

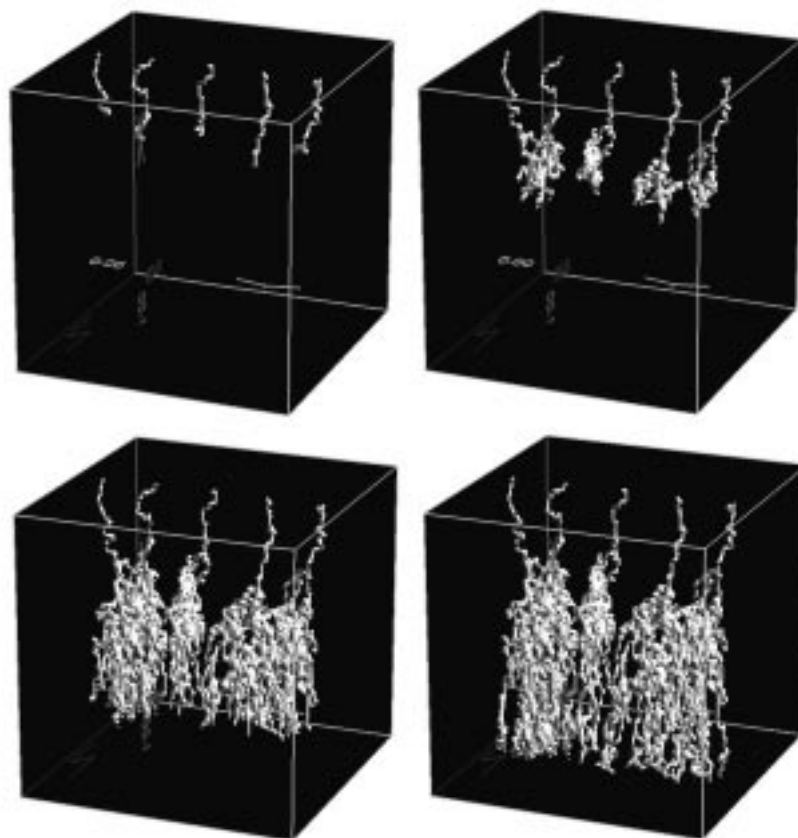


Figure 4. Spatio-temporal evolution of a three-dimensional capillary network towards a single layer (plane) of tumour cells positioned on the bottom face of the cube. There is a gradient of TAF within the tissue, with a high concentration on the bottom face and a lower concentration on the top face. The endothelial cells respond chemotactically to this gradient as well as gradients of fibronectin in the tissue. A branching network is formed which eventually connects with the tumour on the bottom face.

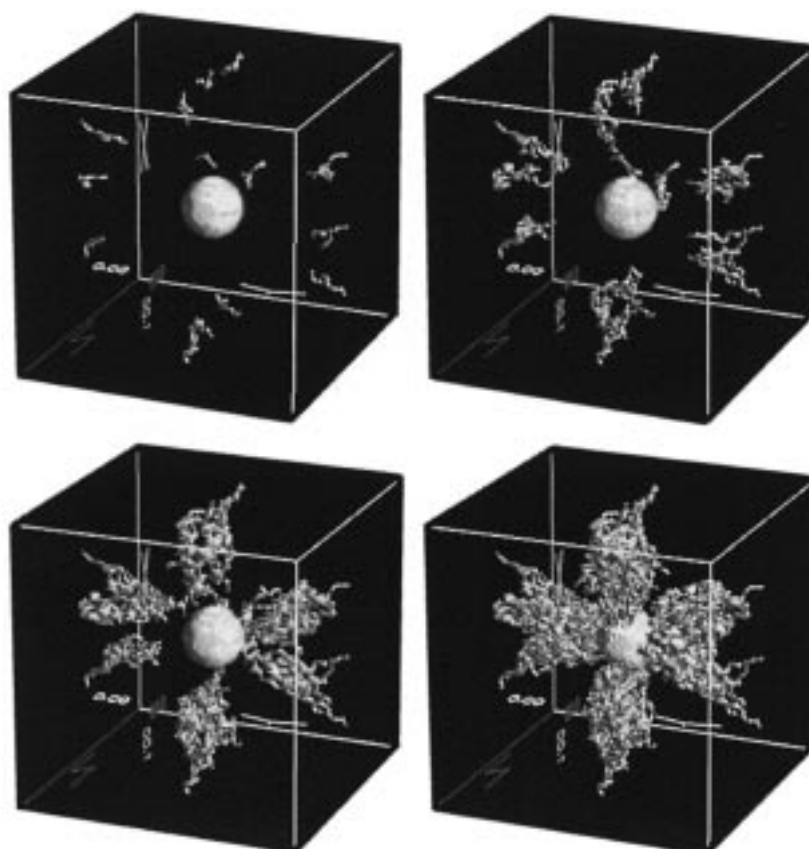


Figure 5. Spatio-temporal evolution of a three-dimensional capillary network towards a central spherical source of tumour cells (cf. avascular tumour or multicell spheroid). There is a gradient of TAF within the tissue, with a high concentration around the central spheroid decaying to lower concentrations in a radially symmetric manner on the boundaries. Once again the endothelial cells respond chemotactically to this gradient as well as gradients of fibronectin in the tissue. A branching network is formed which eventually connects with the avascular tumour in the centre, thus providing the tumour with extra nutrients and opening the way for tumour cells to escape into the blood stream.

anastomose, eventually forming a dense, three-dimensional branched, connected network.

Figure 5 shows four snapshots in time of the capillary network formation in response to the spherical source of tumour cells. At 1 day we see that the initial sprouts have grown a short distance towards the tumour, but have only branched a little. As time progresses, the sprouts begin to branch more and migrate further into the matrix towards the tumour. By 3 days there are sufficient branches for some anastomosis to occur which will lead to a better connected vasculature. In fact, as the sprouts get closer to the tumour the chance of anastomosis occurring rapidly increases. Finally, at 4 days we have connection with tumour and the completion of the angiogenic process. The number of branches rapidly increased between 3 days and 4 days creating a dense

vasculature which almost engulfs the tumour and could be considered as the three-dimensional equivalent of the ‘brush border’.

5. Discussion and conclusions

Mathematical modelling of angiogenesis stretches back a number of years. As new mathematical and computational tools and techniques have developed so has the accuracy and predictive power of the models.

The mathematical model we have focussed on in this chapter is closely linked to experimental results and we have explicitly considered the *tissue response unit* as the basis of our model. Migration of endothelial cells is determined by their response to the local

milieu/microenvironment consisting of cytokines (e.g. VEGF) and matrix molecules (e.g. fibronectin).

The work we have presented here has developed a mathematical model for tumour-induced angiogenesis using a novel blend of continuum, deterministic modelling and discrete, stochastic modelling in both 2 and 3 space dimensions. The model results not only replicate existing experimental protocols (animal cornea models) but also provide a new alternative, non-invasive, predictive three-dimensional ‘assay’. The model results are not only in good qualitative agreement with experimental data but are also in quantitative agreement since parameter values for the models (in particular the length scale L , the cell random motility coefficient D_n , the TAF diffusion constant D_c , the chemotactic coefficient χ_0 and the endothelial cell proliferation rate) have been estimated, as far as possible, from independent experimental measurements, thus grounding the results of the model in a realistic framework.

The discrete model that we presented was derived from a discretized form of the partial differential equations of the continuum model, and permits the tracking of individual endothelial cells located at the capillary sprout-tip. This, in turn, enables the path of the complete capillary sprout to be followed. Since the parameter values used in the discrete model are directly related to those of the continuum model, the results of the simulations of the discrete model are therefore also firmly grounded in a realistic framework. In addition to this, the discrete model enables us to explicitly incorporate rules for the production of new sprouts (branching), the fusion of sprouts to form loops (anastomosis) and sprout extension through endothelial cell proliferation. The results from the discrete model simulations confirm the predictions of the continuum model that both chemotaxis and haptotaxis are necessary for the formation of a capillary network at a large scale.

On a finer scale, the discrete model simulations produce capillary networks with a very realistic structure and morphology, capturing the early formation of loops (anastomosis), the essential dendritic structure of a capillary network and the formation of the experimentally observed ‘brush border’. The discrete model also incorporates a realistic method of modelling mitosis and its effect on the sprouts, i.e. actual extension in the length of the sprout due to cell division.

Although the model has incorporated several key mechanisms involved in the angiogenic process, extensions of the model are of course still possible. For

example, one might consider explicitly modelling more than one angiogenic factor (it is known that some factors induce a mitogenic response while others induce a migratory response). The effect of angiogenic inhibitors may also be considered, as well as more than one matrix macromolecule (e.g. laminin, collagen). However, we believe that these possible extensions are unlikely to provide much more information than is already present (rather they may be considered as ‘fine tuning’).

We believe that a more fruitful direction for the modelling to take is to turn attention to the events occurring at the molecular level and integrate these within the tissue response unit.

For example, several angiogenic factors, e.g. vascular endothelial growth factor (VEGF), acidic and basic fibroblast growth factor (aFGF, bFGF), angiogenin and others, have been isolated [3,5] and *endothelial cell receptors* for these proteins have been discovered [56,60–63]. Indeed, there is now clear experimental evidence that *disrupting these receptors* has a direct effect on the final *structure* of the capillary network [56,61,64,65].

There is now clear experimental evidence that disrupting the transmembrane receptor tyrosine kinases (RTKs) has a direct effect on the structural morphogenesis of the capillary network. Results show that disrupting the RTK Tie2 receptor of endothelial cells leads to a poorly formed capillary network which lacks a full branching structure [56,64,65]. Therefore, the number of active receptors on the cell surface can have a direct influence on outcome of network structure.

Other important aspects of angiogenesis which can be added to the model in the future include incorporating blood flow through the capillary network, with potential application to drug delivery and optimization of chemotherapy regimes; the role of oxygen gradients and oxygen concentration and the role of macrophages. These aspects are also very important to angiogenesis in wound healing.

Notwithstanding these additions, the model already gives very good results. Indeed a recent survey paper of Jain and co-workers [53] discusses the merits and demerits of various angiogenesis assays currently in use both *in vivo* and *in vitro*, e.g. chronic transparent chambers; exteriorized tissue preparations; *in situ* preparations; vascularization into matrix implants; excised tissues; Boyden chamber migration assays; collagen gel assays and proliferation assays. In deciding how effective, efficient and accurate a particular

angiogenesis assay is, Jain et al. [53] identified nine criteria for comparison with an ‘ideal assay’. Specifically, an ideal assay should: (1) provide a knowledge of the release rate and spatio-temporal concentration distribution of angiogenic factors and inhibitors; (2) make use of genetically well-defined neoplastic cells; (3) provide quantitative measurement of the structure of the new vasculature (vascular length, surface area, volume, vessel number, fractal dimension, extent of basement membrane etc.); (4) provide quantitative measurement of the function of the vasculature (i.e. endothelial cell migration rate, proliferation rate, canalization rate, blood flow rate and vascular permeability); (5) be able to distinguish between newly-formed and pre-existing vasculature/vessels; (6) avoid tissue damage; (7) be able to confirm any *in vitro* response *in vivo*; (8) ensure the provision of long-term and non-invasive monitoring; (9) be cost-effective, rapid, easy-to-use, reproducible and reliable.

Comparing our ‘mathematical angiogenesis assay’ with the list of criteria produced by Jain et al. [53] for the ideal angiogenesis assay we find that vessel quantification is highly accurate and easy to do, there is no invasive procedure and no difficulty in ‘setting up the experiment’, there is very little preparation time, and it costs almost nothing as all work is done *in silico*. Experimental replication is easy, as is changing the experimental design, e.g. the tumour size and geometry, the amount of angiogenic factor and/or matrix macromolecules in the system. The mathematical model we have presented and developed also enables one to carry out a quantitative analysis of vascular structures and provides both quantitative structural data (such as vascular length, network surface area, network volume, number of vessels in network, ‘fractal’ dimension) and also quantitative functional data (such as endothelial cell migration rate and proliferation rate). The model could therefore be used as an alternative ‘angiogenesis assay’.

Finally, we note that anti-angiogenesis strategies such as the preferential killing of endothelial cells, the inhibition of endothelial cell proliferation via chemicals such as angiostatin and endostatin [66], the development of anti-chemotactic drugs and the development of anti-haptotactic drugs [67] are now clinically recognized as having enormous potential and promise in the treatment of patients with cancer [68]. In particular, their use as an adjuvant chemotherapy is being recognized as a very effective way to treat secondary tumours (metastases), and mathemati-

cal models of angiogenesis may have an increasingly important role to play in the development and testing of these therapies.

Acknowledgements

This work was supported by BBSRC Grant MMI09008.

References

1. Graham CH, Lala PK: Mechanisms of placental invasion of the uterus and their control. *Biochem Cell Biol* 70: 867–874, 1992
2. Arnold F, West DC: Angiogenesis in wound healing. *Pharmac Ther* 52: 407–422, 1991
3. Folkman J, Klagsbrun M: Angiogenic factors. *Science* 235: 442–447, 1987
4. Folkman J: Tumor angiogenesis. *Adv Cancer Res* 43: 175–203, 1985
5. Folkman J: Angiogenesis in cancer, vascular, rheumatoid and other disease. *Nature Med* 1: 21–31, 1995
6. Folkman J, Brem H: Angiogenesis and inflammation. In: JI Gallin, IM Goldstein, R Snyderman (eds) *Inflammation: Basic Principles and Clinical Correlates* Second Edition. New York: Raven Press, 1992
7. Madri JA, Pratt BM: Endothelial cell–matrix interactions: *in vitro* models of angiogenesis. *J Histochem Cytochem* 34: 85–91, 1986
8. Paweletz N, Knierim M: Tumor-related angiogenesis. *Crit Rev Oncol Hematol* 9: 197–242, 1989
9. Pettet G, Chaplain MAJ, McElwain DLS, Byrne HM: On the role of angiogenesis in wound healing. *Proc Roy Soc Lond B* 263: 1487–1493, 1996
10. Byrne HM, Chaplain MAJ, Pettet GJ, McElwain DLS: A mathematical model of trophoblast invasion. *J Theor Med* 2: 1999
11. Chaplain MAJ, Byrne HM: The mathematical modelling of wound healing and tumour growth: Two sides of the same coin. *Wounds* 8: 42–48, 1996
12. Paku S, Paweletz N: First steps of tumor-related angiogenesis. *Lab Invest* 65: 334–346, 1991
13. Terranova VP, Diflorio R, Lyall RM, Hic S, Friesel R, Maciag T: Human endothelial cells are chemotactic to endothelial cell growth factor and heparin. *J Cell Biol* 101: 2330–2334, 1985
14. Sholley MM, Ferguson GP, Seibel HR, Montour JL, Wilson JD: Mechanisms of neovascularization. Vascular sprouting can occur without proliferation of endothelial cells. *Lab Invest* 51: 624–634, 1984
15. Ausprunk DH, Folkman J: Migration and proliferation of endothelial cells in preformed and newly formed blood vessels during tumour angiogenesis. *Microvasc Res* 14: 53–65, 1977

16. Schor SL, Schor AM, Brazill GW: The effects of fibronectin on the migration of human foreskin fibroblasts and syrian hamster melanoma cells into three-dimensional gels of lattice collagen fibres. *J Cell Sci* 48: 301–314, 1981
17. Hynes RO: *Fibronectins*. New York: Springer-Verlag, 1990
18. Schor AM, Schor SL, Bailey R: Angiogenesis: Experimental data relevant to theoretical analysis. In: Chaplain MAJ, Singh GD, McLachlan JC (eds) *On Growth and Form: Spatio-temporal Pattern Formation in Biology*. Wiley, Chichester, 1999, pp 201–224
19. Albini A, Allavena G, Melchiori A, Giancotti F, Richter H, Comoglio PM, Parodi S, Martin GR, Tarone G: Chemotaxis of 3T3 and SV3T3 cells to fibronectin is mediated through the cell-attachment site in fibronectin and fibronectin cell surface receptor. *J Cell Biol* 105: 1867–1872, 1987
20. Quigley JP, Lacovara J, Cramer EB: The directed migration of B-16 melanoma-cells in response to a haptotactic chemotactic gradient of fibronectin. *J Cell Biol* 97: A450–451, 1983
21. Lacovara J, Cramer EB, Quigley JP: Fibronectin enhancement of directed migration of B16 melanoma cells. *Cancer Res* 44: 1657–1663, 1984
22. McCarthy JB, Furcht LT: Laminin and fibronectin promote the directed migration of B16 melanoma cells *in vitro*. *J Cell Biol* 98: 1474–1480, 1984
23. Carter SB: Principles of cell motility: The direction of cell movement and cancer invasion. *Nature* 208: 1183–1187, 1965
24. Carter SB: Haptotaxis and the mechanism of cell motility. *Nature* 213: 256–260, 1967
25. Bowersox JC, Sorgente N: Chemotaxis of aortic endothelial cells in response to fibronectin. *Cancer Res* 42: 2547–2551, 1982
26. Chaplain MAJ: Avascular growth, angiogenesis and vascular growth in solid tumours: the mathematical modelling of the stages of tumour development. *Mathl Comput Modelling* 23: 47–87, 1996
27. Chaplain MAJ, Anderson ARA: The mathematical modelling, simulation and prediction of tumour-induced angiogenesis. *Invas Metast* 16: 222–234, 1997
28. Anderson ARA, Chaplain MAJ: Continuous and discrete mathematical models of tumor-induced angiogenesis. *Bull Math Biol* 60: 857–899, 1998
29. Chaplain MAJ, Anderson ARA: Modelling the growth and form of capillary networks. In: Chaplain MAJ, Singh GD, McLachlan JC (eds) *On Growth and Form: Spatio-temporal Pattern Formation in Biology*. Wiley, Chichester, 1999, pp 225–249
30. Baum M, Chaplain MAJ, Anderson ARA, Douek M, Vaidya JS: Does breast cancer exist in a state of chaos? *Eur J Cancer* 35: 886–891, 1999
31. Thompson DW: *On Growth and Form*, Cambridge University Press, Cambridge, 1917
32. Zawicki DF, Jain RK, Schmid-Schoenbein GW, Chien S: Dynamics of neovascularization in normal tissue. *Microvasc Res* 21: 27–47, 1981
33. Balding D, McElwain DLS: A mathematical model of tumour-induced capillary growth. *J Theor Biol* 114: 53–73, 1985
34. Chaplain MAJ, Stuart AM: A model mechanism for the chemotactic response of endothelial cells to tumour angiogenesis factor. *IMA J Math Appl Med Biol* 10: 149–168, 1993
35. Byrne HM, Chaplain MAJ: Mathematical models for tumour angiogenesis: numerical simulations and nonlinear wave solutions. *Bull Math Biol* 57: 461–486, 1995
36. Orme ME, Chaplain MAJ: A mathematical model of the first steps of tumour-related angiogenesis: capillary sprout formation and secondary branching. *IMA J Math App Med Biol* 13: 73–98, 1996
37. Anderson ARA, Chaplain MAJ: A mathematical model for capillary network formation in the absence of endothelial cell proliferation. *Appl Math Letters* 11: 109–114, 1998
38. Chaplain MAJ: The mathematical modelling of tumour angiogenesis and invasion. *Acta Biotheor* 43: 387–402, 1995
39. Orme ME, Chaplain MAJ: Two-dimensional models of tumour angiogenesis and anti-angiogenesis strategies. *IMA J Math App Med Biol* 14: 189–205, 1997
40. Chaplain MAJ, Orme ME: Mathematical modelling of tumor-induced angiogenesis. In: Little CD, Mironov V, Sage EH (eds) *Vascular Morphogenesis: In vivo, in vitro, in mente*. Birkhäuser, Boston, 1998, pp 205–240
41. Olsen L, Sherratt JA, Maini PK, Arnold F: A mathematical model for the capillary endothelial cell-extracellular matrix interactions in wound-healing angiogenesis. *IMA J Math Appl Med Biol* 14: 261–281, 1997
42. Mannoussaki D, Lubkin SL, Vernon RB, Murray JD: A mechanical model for the formation of vascular networks *in vitro*. *Acta Biotheor* 44: 271–282, 1996
43. Murray JD, Mannoussaki D, Lubkin SL, Vernon RB: A mechanical theory of *in vitro* vascular network formation. In: Little CD, Mironov V, Sage EH (eds) *Vascular Morphogenesis: In vivo, in vitro, in mente*. Birkhäuser, Boston, 1998, pp 173–188
44. Murray JD, Swanson KR: On the mechanochemical theory of biological pattern formation with applications to wound healing and angiogenesis. In: Chaplain MAJ, Singh GD, McLachlan JC (eds) *On Growth and Form: Spatio-temporal Pattern Formation in Biology*. Wiley, Chichester, 1999, pp 251–285
45. Kiani M, Hudetz A: Computer simulation of growth of anastomosing microvascular networks. *J Theor Biol* 150: 547–560, 1991
46. Landini G, Misson G: Simulation of corneal neovascularization by inverted diffusion limited aggregation. *Invest Ophthalmol Visual Sci* 34: 1872–1875, 1993
47. Nekka F, Kyriacos S, Kerrigan C, Cartilier L: A model of growing vascular structures. *Bull Math Biol* 58: 409–424, 1996
48. Stokes CL, Lauffenburger DA: Analysis of the roles of microvessel endothelial cell random motility and chemotaxis in angiogenesis. *J Theor Biol* 152: 377–403, 1991
49. Gimbrone MA, Cotran RS, Leapman SB, Folkman J: Tumor growth and neovascularization: An experimental model using the rabbit cornea. *J Natn Cancer Inst* 52: 413–427, 1974
50. Muthukkaruppan VR, Kubai L, Auerbach R: Tumor-induced neovascularization in the mouse eye. *J Natn Cancer Inst* 69: 699–705, 1982

51. Little CD, Mironov V, Sage EH (eds): Vascular morphogenesis: *In vivo, in vitro, in mente*. Birkhäuser, Boston, 1998
52. Folkman J, Haudenschild C: Angiogenesis *in vitro*. *Nature* 288: 551–556, 1980
53. Jain RK, Schlenger K, Höckel M, Yuan F: Quantitative angiogenesis assays: Progress and problems. *Nature Med* 3: 1203–1208, 1997
54. Stokes CL, Rupnick MA, Williams SK, Lauffenburger DA: Chemotaxis of human microvessel endothelial cells in response to acidic fibroblast growth factor. *Lab Invest* 63: 657–668, 1990
55. Stokes CL, Lauffenburger DA, Williams SK: Migration of individual microvessel endothelial cells: stochastic model and parameter measurement. *J Cell Sci* 99: 419–430, 1991
56. Hanahan D: Signaling vascular morphogenesis and maintenance. *Science* 227: 48–50, 1997
57. Rupnick MA, Stokes CL, Williams SK, Lauffenburger DA: Quantitative analysis of human microvessel endothelial cells using a linear under-agarose assay. *Lab Invest* 59: 363–372, 1988
58. Bray D: *Cell Movements*. Garland Publishing, New York, 1992
59. Williams SK: Isolation and culture of microvessel and large-vessel endothelial cells; their use in transport and clinical studies. In: McDonagh P (ed) *Microvascular Perfusion and Transport in Health and Disease*. Karger, Basel, 1987, pp 204–245,
60. Duh EJ, King GL, Aiello LP: Identification of a VEGF receptor (KDR/FLK) promoter element which binds an endothelial cell-specific protein conferring endothelial selective expression. *Invest Ophthalmol Vis Sci* 38: 1124–1125, 1997
61. Dumont DJ, Gradwohl G, Fong GH, Puri MC, Gertsenstein M, Auerbach A, Breitman ML: Dominant-negative and targeted null mutations in the endothelial receptor tyrosine kinase, TEK, reveal a critical role in vasculogenesis of the embryo. *Genes Dev* 8: 1897–1909, 1994
62. Fong GH, Rossant J, Gertsenstein M, Breitman ML: Role of the FLT-1 receptor tyrosine kinase in regulating the assembly of vascular endothelium. *Nature* 376: 66–70, 1995
63. Hewett PW, Murray JC: Coexpression of FLT-1, FLT-4 and KDR in freshly isolated and cultured human endothelial-cells. *Biochem Biophys Res Commun* 221: 697–702, 1996
64. Millauer B, Wizigman-Voos Schnürch H, Martinez R, Müller NPH, Risau W, Ullrich A: High-affinity VEGF binding and developmental expression suggest FLK-1 as a major regulator of vasculogenesis and angiogenesis. *Cell* 72: 835–846, 1993
65. Sato TN, Tozawa Y, Deutsch U, Wolburgbuchholz K, Fujiwara Y, Gendronmaguire M, Gridley T, Wolburg H, Risau W, Qin, Y: Distinct roles of the receptor tyrosine kinases TIE-1 and TIE-2 in blood-vessel formation. *Nature* 376: 70–74, 1995
66. O'Reilly MS, Holmgren L, Shing Y, Chen C, Rosenthal RA, Moses M, Lane WS, Cao Y, Sage EH, Folkman J: Angiostatin: A novel angiogenesis inhibitor that mediates the suppression of metastases by a Lewis lung carcinoma. *Cell* 79: 315–328, 1994
67. Yamada KM, Olden K: Fibronectin-adhesive glycoproteins of cell surface and blood. *Nature* 275: 179–184, 1978
68. Harris AL: Antiangiogenesis for cancer therapy. *Lancet* 349 (Suppl II): 13–15, 1997

Address for offprints: Mark Chaplain, Department of Mathematics, University of Dundee, Dundee DD1 4HN, UK; Tel.: 01382-345369; Fax: 01382-345516; E-mail: chaplain@maths.dundee.ac.uk